Ground Fissure Identification in Mining Areas from UAV Images Based on DN-CAMSCBNet

Haibin Hu[1,*], Xinhui Guo[2], Jie Xiao[2]
[1]*School of Traffic Engineering, Shanxi Vocational University of Engineering Science and Technology, Jinzhong Shanxi 030619, China*
[2]*Shanxi Institute of Surveying and Mapping Geographic Information, Taiyuan Shanxi 030001, China*
[*]*sxty555321@sina.com; 105348910@qq.com; xiaojie19801208@163.com*

***Abstract*—The development and use of mine resources have had many adverse impacts on the environment of mining areas. Among them, ground fissures are the most serious. They not only threaten the ecological protection of mining areas but also hinder the sustainable exploitation of energy. To mitigate the damage to the ecological environment caused by mining areas and ensure sustainable long-term resource exploitation, it is of particular importance to identify ground fissures in mining areas efficiently. Therefore, this paper proposes a ground fissure identification model for UAV images in mining areas named DN-CAMSCBNet. This method integrates the channel attention mechanism and the dropout mechanism on the basis of the traditional U-Net. Meanwhile, it introduces the multiscale convolution block and Nesterov-accelerated adaptive moment estimation. These are used to enhance its ability to capture complex image features, expand the receptive field of the original model, reduce the number of parameters, and reduce computational complexity. To verify the segmentation performance of the model, it is compared with U-Net, D-CAMNet, and D-MSCBNet models. The experimental results show that the accuracy and precision of the DN-CAMSCBNet model can reach 99.47 % and 92.25 %, respectively, and the F1 score is 0.7699. All these are superior to comparison models and can provide strong support for the identification of ground fissures in mining areas.**

***Index Terms*—Mine ground fissures; UAV images; U-Net; Multiscale convolution block; Channel attention mechanism.**

I. INTRODUCTION

Coal mining has played a significant role in alleviating the global energy shortage and promoting economic growth. However, it has also caused a series of severe negative impacts on mining areas and their surrounding environments. Ground fissures, in particular, have become a common and highly harmful geological disaster. In numerous mining regions, surface facilities, and buildings have suffered extensive damage. For example, in a certain mining area, it was reported that over 50 % of the surface structures showed signs of damage due to ground fissures within a five-year period. This not only disrupts the ecological environment, but also poses a direct threat to the lives and property of local residents [1]–[5]. Therefore, the accurate and timely identification of ground fissures in mining areas is of utmost importance for disaster prevention, economic loss reduction, and ecological environment protection.

Traditionally, for the detection of large ground fissures, geophysical exploration techniques have been widely used. These methods rely on complex equipment and extensive field operations. For instance, seismic surveys require the deployment of a large number of sensors over a wide area, which requires significant human and material resources. The process is time-consuming, with an average survey taking several weeks to complete, and the costs are extremely high. Moreover, achieving comprehensive monitoring of large-scale mining areas is a daunting task. Even worse, when it comes to minute fissures, these techniques often fail to provide accurate results [6]. In contrast, satellite remote sensing technology offers a broad coverage and rich spectral information, allowing large-scale ground fracture detection [7]–[9]. However, due to the limitations of satellite orbits and sensor resolutions, satellite images have difficulties in precisely identifying tiny fissures. In practical applications, the time interval between image acquisitions is often too long to capture the dynamic changes of ground fissures in a timely manner, thus restricting its effectiveness in detailed fissure detection [10].

With the continuous progress of science and technology, unmanned aerial vehicle (UAV) technology has emerged as a promising alternative for the ground fissure identification. UAVs are highly maneuverable and can access areas that are difficult for traditional survey methods. Their data acquisition process is relatively simple and cost-effective. For example, a single UAV flight can cover a large area in a short time, and the high-resolution images it captures can reach the centimetre level, allowing detailed detection of ground fissures [11]–[13]. The application of UAV remote sensing technology has greatly accelerated the pace of fissure information collection, improving work efficiency, and providing more accurate data for analysis [14].

In recent years, with the continuous development of deep learning technology, more and more studies have applied it to the field of remote sensing to achieve the identification and detection of ground objects. The identification of ground fissures based on UAV images and deep learning has become

Manuscript received 15 October, 2024; accepted 29 December, 2024.
This research has been supported by the National Natural Science Foundation of China under Grant No. U21A20107; Fundamental Research Program of Shanxi Province under Grant. No. 202203021211156.

a research hotspot at present, providing new ideas for solving the problem of ground fissure monitoring in complex environments. This method breaks through the limitations of traditional manual detection and simple image analysis, greatly improving detection efficiency and accuracy. For example, Jiang *et al.* [15] proposed a deep learning model MFPA-Net based on an encoder-decoder framework to automatically extract ground fissures in UAV images. W. Luo, Hao, Chen, Zhang, Wang, and Li [16] proposed a deep learning network, PF-Unet3+ to extract ground fissures. Tao *et al.* [4] developed an automatic recognition method based on deep learning to realise efficient recognition and extraction of fissures in UAV images. Yuan, Zhang, Han, and Liang [17] proposed a semantic segmentation algorithm suitable for the detection of fissures based on the DeepLabv3+.

To address these challenges, this paper focusses on the identification of ground fissures in mining areas. We propose the DN-CAMSCBNet model, which is an improvement over the traditional U-Net model. The U-Net model has been widely used in image segmentation tasks due to its unique architecture that combines an encoder for feature extraction and a decoder for image reconstruction. However, in the context of the mining area ground fissure identification, it has certain limitations. Our proposed model integrates the channel attention mechanism (CAM), which enables the model to adaptively focus on the most relevant channels of the input image. By assigning different weights to each channel, the model can enhance the representation of important features and suppress noise. For example, in the presence of complex backgrounds and various types of ground cover in the mining area, CAM can help the model to better distinguish the features of ground fissures from other objects.

In addition, we introduce the dropout mechanism. During the training process, the dropout mechanism randomly deactivates a certain proportion of neurons in each layer. This helps prevent the model from overfitting, especially in the complex and diverse environment of the mining area, where the data distribution may be highly variable. By reducing the interdependence between neurons, the model can learn more robust and generalisable features, thus improving its performance on unseen data.

Furthermore, we incorporate the multiscale convolution block (MSCB). The MSCB utilises multiple convolution kernels of different sizes to extract features at different scales. In the mining area, ground fissures can vary in size and shape. The MSCB allows the model to capture both fine-grained details and coarse-grained structures of the fissures, providing a more comprehensive and accurate representation of the ground fissures. This is crucial to accurately identify and segment ground fissures in different scenarios.

By integrating these components into the U-Net model, the DN-CAMSCBNet model is designed to enhance the accuracy and efficiency of ground fissure identification in mining areas. It can better handle complex geological conditions, diverse surface features, and various types of ground fissures in the mining area, providing strong support for safe mining operations and effective ecological environment management.

II. Research Area and Data

A. Overview of the Research Area

The research area is located in the Huipodi Coal Mine, Hongtong County, Linfen City, Shanxi Province. It lies in the northwest of Hongtong County and the southwest of Fenxi County in Shanxi Province. It is approximately 25 kilometres from the county seat of Hongtong in a straight line. It extends from Chaijiayuan Village, Liujiayuan Town, Hongtong County in the north to Dagucun Village in the south, from Xiaogucun Village in the west to Jiacun Village, Heping Town, Fenxi County in the east. The range of geographical coordinates (CGCS2000 National Geodetic Coordinate System) is from 111°28′45.811″ east longitude to 111°35′26.794″ east longitude, and from 36°25′49.270″ north latitude to 36°30′02.890″ north latitude. The coordinates of the central point are 111°31′20.492″ east longitude and 36°27′06.810″ north latitude. The mining area is located in the low-mountain and loess hilly area. It has a warm-temperate monsoon-type continental climate with four distinct seasons and a relatively large temperature difference between day and night. In spring, it is windy and rainless; in summer, rainfall is concentrated; in autumn, the sky is clear and the air is crisp; in winter, it is cold with little snow. The surface water of the coal mine belongs to the Fenhe River system in the Yellow River Basin. There are no large surface water systems in the mining area, only several seasonal gullies. During the rainy season, each gully receives atmospheric precipitation that gathers into torrents. The torrents flow south into the Houdian River in Hongtong County and then southeast through Xucun in Hongtong County to the Fenhe River. The development of Huipodi Coal Mine has caused large-scale damage to the land. During the mining process, geological disasters such as landslides, mudslides, ground subsidence, and ground fissures have been triggered. Among them, during the underground mining process, the continuous excavation of ores has led to the formation of large areas of goaf underground. These goafs usually lack sufficient support, causing the surface rock strata to gradually subside and generate fissures. As the goaf area expands, the scope of surface subsidence and the number of fissures gradually increase.

B. Data Sources

On 26 September 2024, data collection was performed using the DJI Mavic 3e UAV. The specific parameters of the UAV highlight its exceptional capabilities in certain aspects when compared to some commonly used drones. The camera equipped on this UAV has an effective pixel of 20 million, substantially surpassing many standard drones in the market, enabling it to capture more detailed and clearer images. Additionally, its field-of-view angle of 84 ° provides a broader perspective, allowing for the capture of more comprehensive data during each flight. Moreover, the image data contain complete POS information, including position and attitude angle data, ensuring that the images have relatively high positioning accuracy. The specific parameters are shown in Table I.

When collecting data, according to the range of the survey area and the elevation data, flight path design software was

used to design the flight path by combining the elevation of the lowest and highest points in the survey area, showcasing the advanced planning and execution capabilities of the DJI Mavic 3e UAV. Using Agisoft Photoscan Professional UAV data processing software, the images collected were stitched together to generate a map of the mining area survey area that meets the accuracy requirements of 1:1000, as shown in Fig. 1.

TABLE I. RELATED PARAMETERS OF UAV.

Parameters of DJI Mavic 3e UAV	
Type	Rotor
Bare Machine Weight	915 g
Maximum Takeoff Weight	1050 g
Weight	12.5 kg
Maximum Ascending Speed	6 m/s
Maximum Descending Speed	6 m/s
Maximum Flight Time	45 minutes
Maximum Hover Time	38 minutes
Maximum Flight Range	32 km

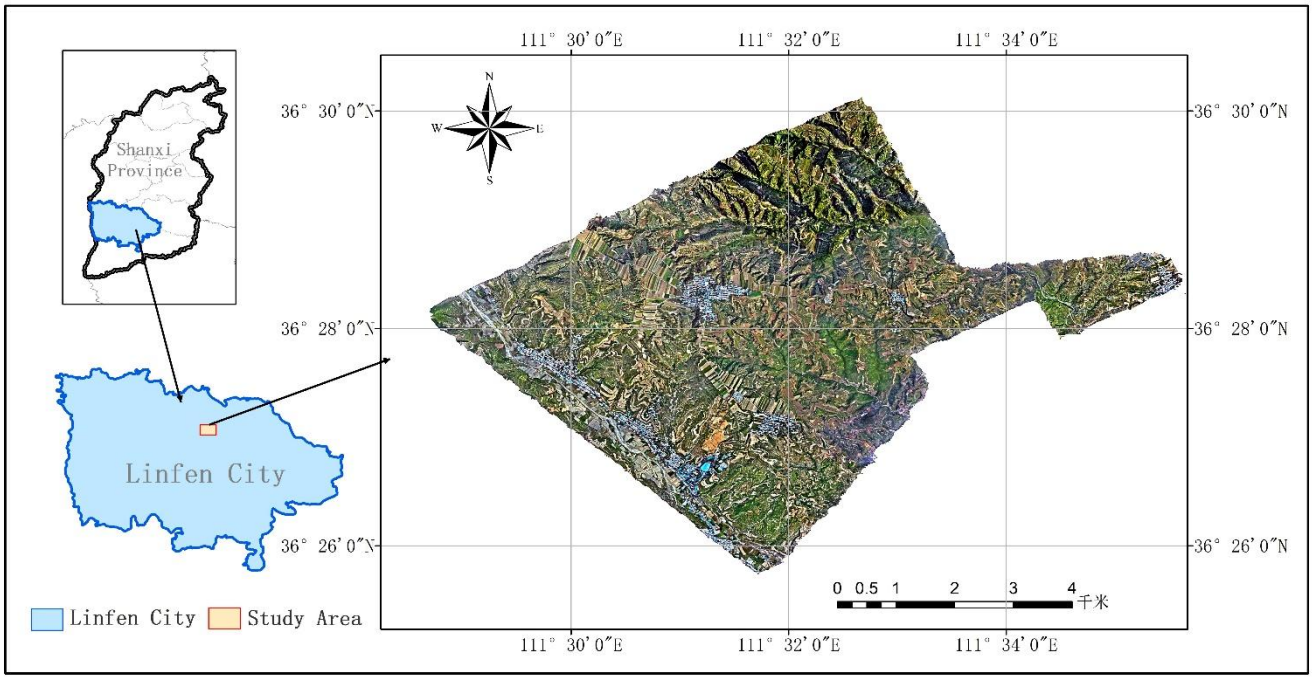

Fig. 1. Research area.

C. *Production of Data Set*

To ensure that the images meet the training requirements of the model, the OpenCV library was used to standardise the size of the selected UAV images. The images were segmented into images with a size of 512×512 pixels. However, after image segmentation, many poor quality image data were generated. The problems are not included in the ground fissure target, incomplete ground fissure target, and low image definition. To create a high-quality data set, this study selected 50 images that were highly clear and contained a relatively large number of detection targets. The study then utilised the LabelMe image annotation tool in Python to annotate the ground fissures within these images. Following annotation, the generated JSON files were converted to the JPG format, which matches the format of the original images. The data set was expanded to 200 images using image enhancement techniques. And the data set was randomly divided into a training set, a testing set, and a validation set, with the proportion set as 7:2:1. Finally, 140 training set images, 40 validation set images, and 20 testing set images were obtained. The data set preprocessing process is shown in Fig. 2.

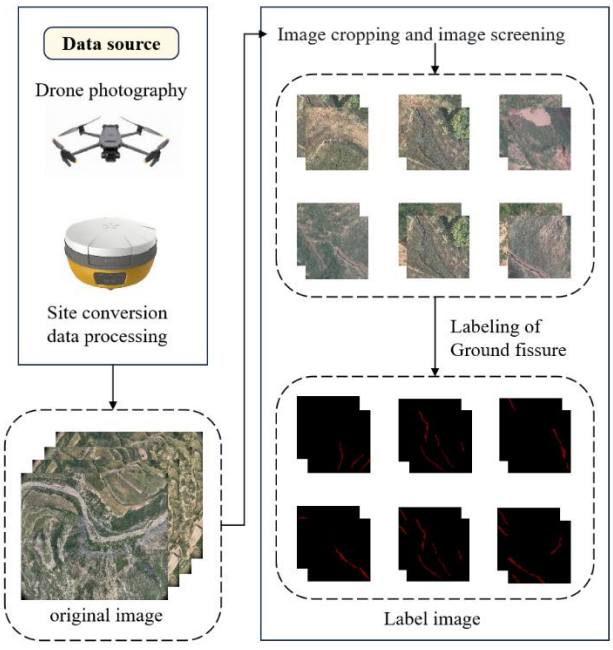

Fig. 2. Data set preprocessing process.

III. RESEARCH METHODS

Images of a large area of the mining area can be obtained quickly using UAV images. Based on the DN-CAMSCBNet model, this paper has achieved the rapid detection of ground fissures in drone images of the mining area. The specific methods are shown in Fig. 3. First, data collection is carried out using drones. Then, the collected data are preprocessed, including operations like data enhancement. After that, the data set is randomly divided to construct the ground fissure data set, which is then used for the training of the model. Finally, the effects of the DN-CAMSCBNet model on ground fissure extraction are compared with those of the three traditional methods, namely U-Net, D-CAMNet, and D-MSCBNet. Through evaluation indicators such as Precision, Accuracy, Recall, and F1 score, the detection effects of various methods are evaluated.

A. U-Net

The U-Net network model is fundamental to image segmentation [18]. It was first proposed in 2015 and was initially intended for medical image segmentation. After many improvements, it is widely used in various fields such as remote sensing, medical imaging, and geological disaster monitoring. Named for its U-shaped architecture, its structure comprises a contracting path (encoder) and a symmetric expanding path (decoder). The encoder extracts image features via a series of convolution and pooling operations, reducing image resolution while increasing feature channels to capture high-level semantic info. The decoder restores image resolution by mapping the semantic information learnt by the encoder to the spatial resolution of the original image, achieving pixel-level segmentation. The network structure has many feature reuse and skip connection mechanisms. These can directly transfer low-level features (such as edge and texture details) from the encoder's earlier layers to the decoder. This design allows the decoder to fully use low-level features when restoring resolution, yielding more accurate segmentation results. See Fig. 4 for the schematic of the network structure.

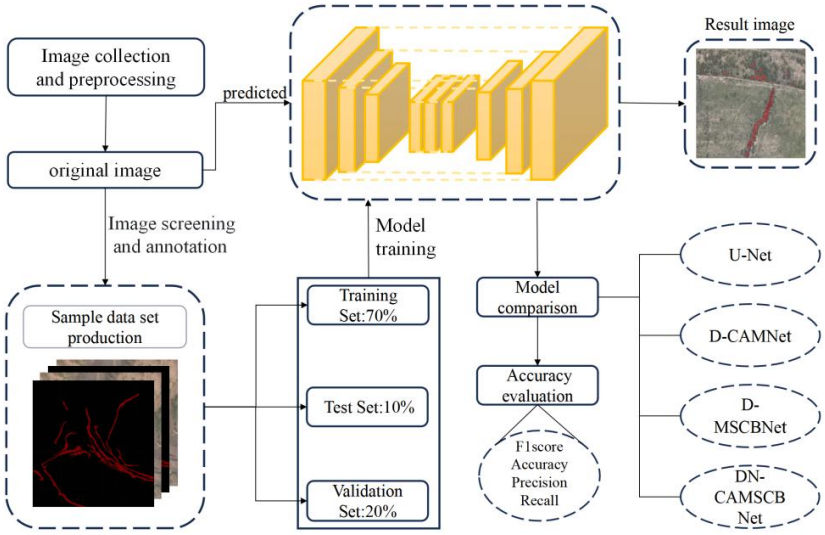

Fig. 3. Technology roadmap.

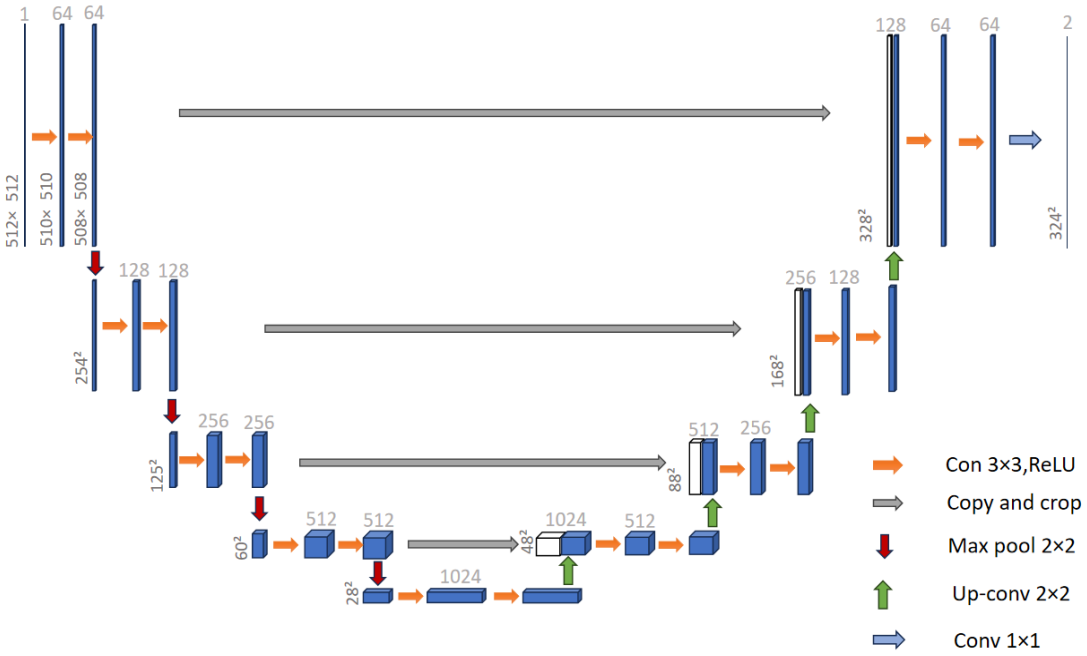

Fig. 4. U-Net structure.

B. Channel Attention Mechanism

CAM, a technique in deep learning, enhances the representation of features of neural networks, widely used especially in computer vision. Its core is to dynamically assign importance weights to each channel based on the characteristics of the input data [19]–[21]. Different channels usually contain different semantic information, and some of these channels may be more crucial to the current task. While other channels may contain noise or irrelevant information, the model enhances its overall performance by assigning varying weights to the channels, thereby focussing more on valuable features.

C. Multiscale Convolutional Block

MSCB is a convolution operation module used for extracting multiscale features. Its goal is to enable neural networks to extract image features at different scales, thus better addressing various complex visual tasks. By using different-sized convolutional kernels in multiple branches, the model is able to capture multilevel features from fine-grained (small kernel) to coarse-grained (large kernel), achieving a more comprehensive data representation. By combining different convolution kernels reasonably, the computational load and model complexity can be controlled to a certain extent, and the robustness of the model can be enhanced. In image segmentation, MSCB can more precisely distinguish object and region boundaries at different scales, improving segmentation accuracy. Specifically, a 3×3 convolution kernel is mainly used to adjust the number of channels and capture local features. Larger convolution kernels, such as 7×7 and 5×5 can capture more extensive local area features, covering pixel information within different ranges. Specific calculation formulas are shown in (1) and (2) as follows:

$$M_c = \sigma(MLP[AvgPool(F)] + MLP[MaxPool(F)]), \quad (1)$$

$$F' = M_c \odot F. \quad (2)$$

Among them, F represents the input feature map, FS is the feature map after applying a convolution kernel of a certain size, and F' is the concatenated output of different convolution kernel sizes.

D. Dropout Mechanism and Nadam Optimiser

To solve the overfitting problem likely in complex mining area environment, this paper uses the dropout mechanism and the Nadam optimiser. Dropout is a widely used regularisation technique in the neural network training process. Its basic idea is to randomly "drop out" some neurons in each training iteration, reducing the model's dependence on specific neurons during the training process. This enables the neural network to learn more robust and representative features, thereby enhancing the generalisability of the model. The Nadam optimiser is an improved optimisation algorithm. It combines the advantages of the Nesterov-accelerated gradient method and the Adam optimiser. During the update process, Nadam takes both the first-order moment and the second-order moment into account, and utilises these estimates to adjust the update direction and step length of the weights. When updating the weights, Nadam utilises an adaptive learning rate that dynamically adjusts based on estimates of both the first-order moment and the second-order moment, enabling faster and more stable convergence.

E. Construction of the DN-CAMSCBNet Model

Based on the U-Net network, this paper introduces CAM, MSCB, the dropout mechanism, and the Nadam optimiser to construct a semantic segmentation model named DN-CAMSCBNet. Its structure is shown in Fig. 5.

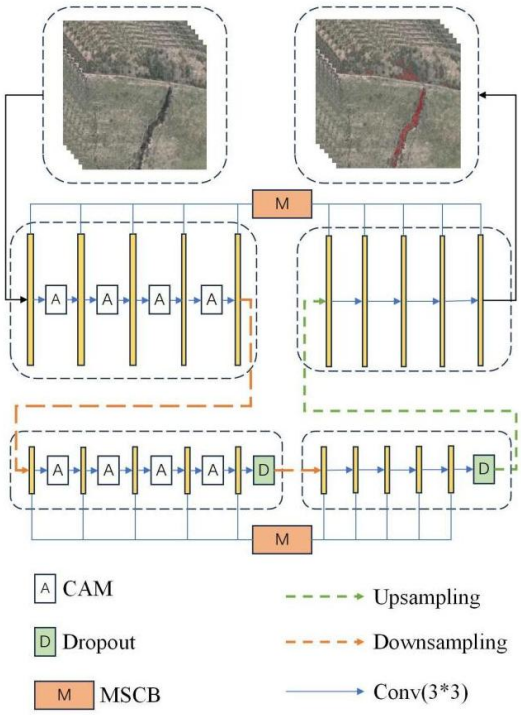

Fig. 5. Structural diagram of the DN-CAMSCBNet model.

In the encoder stage, the input image first undergoes convolution to extract local features. Then activation functions are applied to introduce nonlinearity and increase the expressive ability of the model. Then, use the max-pooling operation to lower the image resolution and make the features more abstract. In this process, the dropout mechanism is also used. It randomly produces the output of neurons 0 with a certain probability to prevent overfitting effectively. In the decoder stage, the up-sampling operation is performed first, and the resolution of the image is gradually recovered. The feature map of the corresponding resolution is then spliced with the encoder to obtain more details. Subsequently, the transposed convolution operation enhances the image's resolution, followed by the application of an activation function to introduce nonlinearity. Then, conduct convolution and activation operations again to further adjust and fuse the features, making the output feature map closer to the final segmentation result. Overall, these improvements help to improve segmentation accuracy, speed up model convergence, better handle occlusion and terrain complexity, and make ground fissure identification in mining areas more accurate in different environments. In addition, the model has a flexible structure and can be adjusted for different tasks and data sets.

IV. EXPERIMENTS AND ANALYSIS

A. Experimental Environment

In terms of hardware environment, the GPU used is an NVIDIA GeForce RTX 4060 Laptop GPU, and the CPU is an Intel(R) Core (TM) i7-14650HX. The operating system is Windows 11. The deep learning framework used is TensorFlow version 2.10.0, with Python version 3.8. The accelerated platform is CUDA version 12.4.

B. Evaluation Metrics

To comprehensively and effectively evaluate the segmentation performance of the model, this paper selects four commonly used evaluation metrics: Precision, Accuracy, Recall, and F1 Score. The calculation methods for these metrics are as follows:

$$Precision = \frac{TP}{TP + FP}, \tag{3}$$

$$Accuracy = \frac{TP + TN}{TP + TN + FP + FN}, \tag{4}$$

$$Recall = \frac{TP}{TP + FN}, \tag{5}$$

$$F1 = \frac{2 \times Precision \times Recall}{Precision + Recall}. \tag{6}$$

Here, TP, FP, FN, and TN represent True Positive, False Positive, False Negative, and True Negative, respectively, as shown in the confusion matrix in Table II.

TABLE II. CONFUSION MATRIX.

	Actually Positive	**Actually Negative**
Predicted Positive	TP	FN
Predicted Negative	FP	TN

C. Experimental Results and Analysis

To verify the feasibility of the proposed method in open-pit mine ground fissure identification. Conduct tests on the data set constructed above under the same configuration conditions of the experimental environment. The model parameters were set as follows: each batch contains 16 randomly ordered images, the number of image training epochs is 16 and the initial learning rate of 0.001.

The base U-Net model was used to identify ground fissures in the mine. Additionally, ablation experiments were performed. CAM and MSCB were removed separately from the final model, DN-CAMSCBNet, resulting in two new models: D-CAMNet and D-MSCBNet. The accuracy results for these four methods are shown in Table III.

TABLE III. ACCURACY EVALUATION RESULTS.

Method	**Precision**	**Accuracy**	**Recall**	**F1-Score**
U-Net	81.62 %	99.05 %	14.57 %	0.2473
D-CAMNet	86.51 %	98.98 %	20.34 %	0.3276
D-MSCBNet	90.75 %	98.84 %	53.25 %	0.6708
DN-CAMSCBNet	92.25 %	99.47 %	65.86 %	0.7699

The results in Table III show that the DN-CAMSCBNet model performs best across all evaluation metrics. It achieved a Precision of 92.25 %, Accuracy of 99.47 %, Recall of 66.28 %, and F1 Score of 0.7699. Compared to the D-MSCBNet model, DN-CAMSCBNet improved Precision, Accuracy, Recall, and F1 Score by 1.5 %, 0.63 %, 12.61 %, and 9.91 %, respectively. Compared to D-CAMNet, these metrics increased by 5.74 %, 0.49 %, 45.52 %, and 44.23 %. Finally, compared to the base U-Net model, DN-CAMSCBNet achieved improvements of 10.63 %, 0.42 %, 51.29 %, and 52.26 %, respectively. These results validate the effectiveness of the improved model, showing that it helps the computer to learn and identify objects more accurately. It demonstrates a clear advantage in identifying ground fissures in UAV images of mining areas.

The training and validation losses of the four models during training are shown in Fig. 6. From the figure, it is evident that the DN-CAMSCBNet model has a faster convergence rate and reaches the lowest loss value within the same number of training iterations. Compared to the U-Net model, which has the lowest accuracy, D-CAMNet captures more features through CAM, thus improving its performance. D-MSCBNet further enhances the results with additional convolution layers but still lags behind DN-CAMSCBNet. By combining CAM and MSCB, DN-CAMSCBNet efficiently captures finer and broader feature details. Its faster convergence speed also underscores its superior performance in identifying ground fissures in UAV images of mining areas.

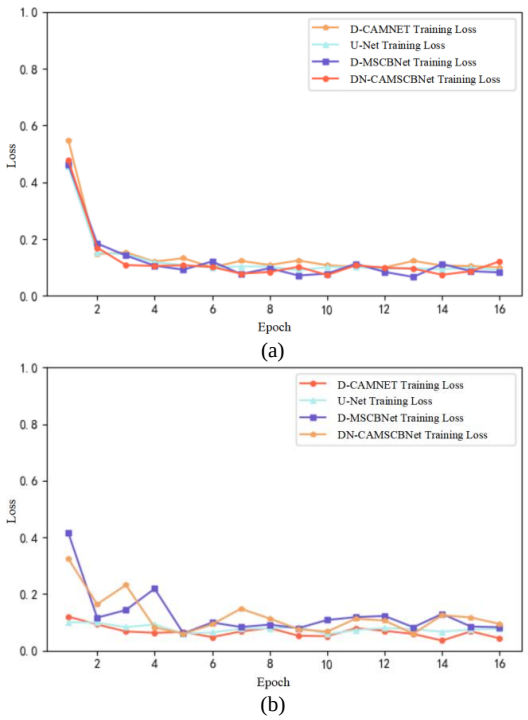

Fig. 6. (a) Training losses and (b) validation losses of four models on training sets.

The visual results of ground fissure identification for the four models are shown in Fig. 7. As seen in the figure, the original U-Net model has a certain capability for fissure identification, but lacks precision in capturing details. Its results may appear relatively simplistic, making it difficult to accurately identify more complex or fine fissure regions. In comparison, D-CAMNet and D-MSCBNet show improved identification performance, although they still fall short in some details compared to the enhanced DN-CAMSCBNet. The DN-CAMSCBNet model excels at extracting fine fissure details while effectively filtering out noise.

Combining the identification results from different scenes in Fig. 7 with the evaluation metrics in Table III, it is clear that the DN-CAMSCBNet model demonstrates superior performance. This is reflected in its higher Precision, Accuracy, Recall, and F1 Score. The results indicate that DN-CAMSCBNet outperforms the traditional U-Net model and many other improved models.

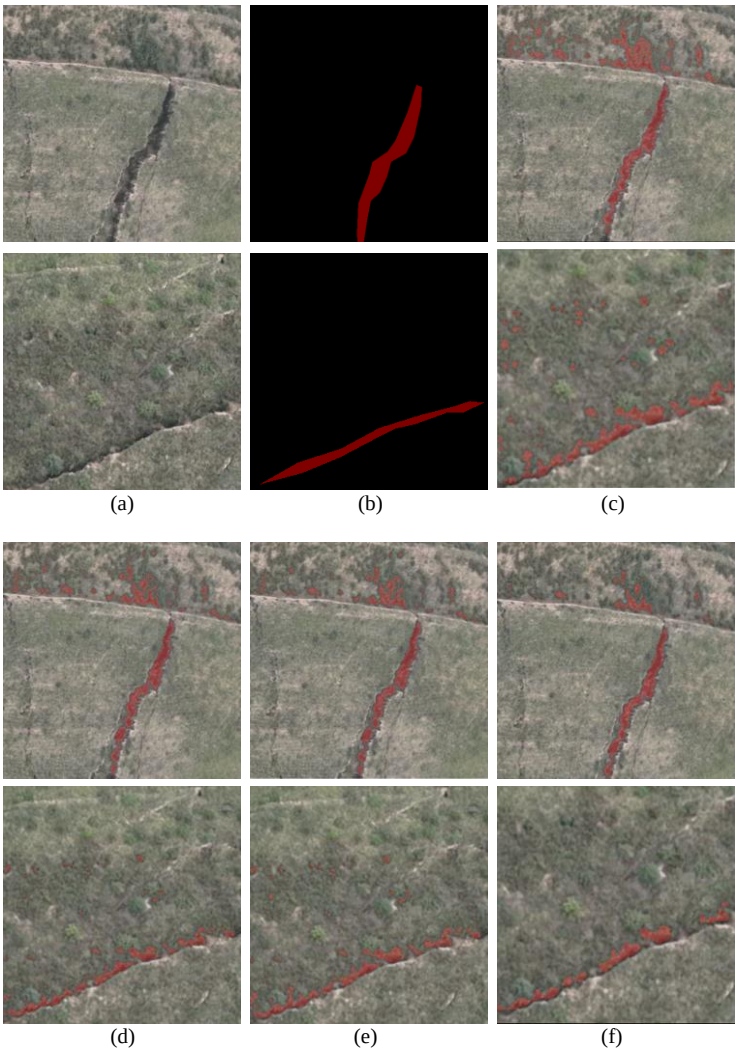

Fig. 7. Results of identification of different models in ground fissures: (a) Original image; (b) Labels; (c) U-net; (d) D-CAMNet; (e) D-MSCBNet; (f) DN-CAMSCBNet.

V. CONCLUSIONS

To address the challenge of rapid and accurate identification of ground fissures in mining areas, this paper proposes the semantic segmentation model DN-CAMSCBNet. By integrating the channel attention mechanism (CAM) and multiscale convolutional block (MSCB), and introducing the dropout mechanism and Nadam optimiser, the model expands the receptive field while reducing parameters and complexity. Experimental results demonstrate the superior performance of the DN-CAMSCBNet model in ground fissure identification.

Specifically, on a data set that contains 200 images, DN-CAMSCBNet significantly outperforms D-MSCBNet, D-CAMNet, and the traditional U-Net model in terms of Precision, Accuracy, Recall, and F1 score. In detail, DN-CAMSCBNet achieves a Precision of 92.25 %, an Accuracy of 99.47 %, a Recall of 66.28 %, and an F1 score of 0.7699. Compared to D-MSCBNet, DN-CAMSCBNet improves these metrics by 1.5 %, 0.63 %, 12.61 %, and 9.91 %, respectively. Compared to D-CAMNet, these improvements are 5.74 %, 0.49 %, 45.52 %, and 44.23 %, respectively. And compared to the U-Net model, DN-CAMSCBNet enhances Precision, Accuracy, Recall, and F1 score by 10.63 %, 0.42 %, 51.29 %, and 52.26 %, respectively.

These numerical data fully demonstrate the superiority of the DN-CAMSCBNet model in ground fissure identification. The model is effective in not only capturing the fine features of ground fissures, but also it performs well in processing tiny cracks. Therefore, the DN-CAMSCBNet model provides a new solution for the rapid and accurate identification of ground fissures in mining areas, offering broad application prospects.

CONFLICTS OF INTEREST

The authors declare that they have no conflicts of interest.

REFERENCES

[1] M. Zang, J. Peng, N. Xu, and Z. Jia, “A probabilistic method for mapping earth fissure hazards”, *Scientific Reports*, vol. 11, art. 8841, 2021. DOI: 10.1038/s41598-021-87995-1.

[2] Y. Li, H. Liu, L. Su, S. Chen, X. Zhu, and P. Zhang, “Developmental features, influencing factors, and formation mechanism of underground mining–induced ground fissure disasters in China: A review”, *International Journal of Environmental Research and Public Health*,

vol. 20, no. 4, 2023. DOI: 10.3390/ijerph20043511.
[3] Y. Fu, Y. Wu, and X. Yin, "A study on the movement and deformation law of overlying strata and the self-healing characteristics of ground fissures in non-pillar mining in the aeolian sand area", *Sustainability*, vol. 15, no. 20, art. 15136, 2023. DOI: 10.3390/su152015136.
[4] T. Tao *et al.*, "Identification of ground fissure development in a semi-desert aeolian sand area induced from coal mining: Utilizing UAV images and deep learning techniques", *Remote Sensing*, vol. 16, no. 6, art. 1046, 2024. DOI: 10.3390/rs16061046.
[5] K. Yang *et al.*, "Automated extraction of ground fissures due to coal mining subsidence based on UAV photogrammetry", *Remote Sensing*, vol. 14, p. 1071, 2022. DOI: 10.3390/rs14051071.
[6] Y. Zhao *et al.*, "Identification of mining induced ground fissures using UAV and infrared thermal imager: Temperature variation and fissure evolution", *ISPRS Journal of Photogrammetry and Remote Sensing*, vol. 180, pp. 45–64, 2021. DOI: 10.1016/j.isprsjprs.2021.08.005.
[7] J. Peng *et al.*, "Distribution and generative mechanisms of ground fissures in China", *Journal of Asian Earth Sciences*, vol. 191, art. 104218, 2020. DOI: 10.1016/j.jseaes.2019.104218.
[8] Z. Zhou, X. Yao, K. Ren, and H. Liu, "Formation mechanism of ground fissure at Beijing Capital International Airport revealed by high-resolution InSAR and numerical modelling", *Engineering Geology*, vol. 306, art. 106775, 2022. DOI: 10.1016/j.enggeo.2022.106775.
[9] F. Zhao, W. Gong, H. Tang, S. Pudasaini, T. Ren, and Z. Cheng, "An integrated approach for risk assessment of land subsidence in Xi'an, China using optical and radar satellite images", *Engineering Geology*, vol. 314, art. 106983, 2023. DOI: 10.1016/j.enggeo.2022.106983.
[10] Y. Fu *et al.*, "Ground fracture development and surface fracture evolution in N00 method shallowly buried thick coal seam mining in an arid windy and sandy area: A case study of the Ningtiaota Mine (China)", *Energies*, vol. 14, no. 12, pp. 1–18, 2021. DOI: 10.3390/en14227712.
[11] H. Jia, B. Wei, G. Liu, R. Zhang, B. Yu, and S. Wu, "A Semi-automatic method for extracting small ground fissures from loess areas using unmanned aerial vehicle images", *Remote Sensing*, vol. 13, no. 9, art. 1784, 2021. DOI: 10.3390/rs13091784.
[12] F. Zhang, Z. Hu, Y. Fu, K. Yang, Q. Wu, and Z. Feng, "A new identification method for surface cracks from UAV images based on machine learning in coal mining areas", *Remote Sensing*, vol. 12, no. 10, art. 1571, 2020. DOI: 10.3390/rs12101571.
[13] Y. Liang, F. Zhang, K. Yang, and Z. Hu, "A surface crack damage evaluation method based on kernel density estimation for UAV images", *Sustainability*, vol. 14, no. 23, p. 16238, 2022. DOI: 10.3390/su142316238.
[14] X. Li, "Ship segmentation via combined attention mechanism and efficient channel attention high-resolution representation network", *Journal of Marine Science and Engineering*, vol. 12, no. 8, p. 1411, 2024. DOI: 10.3390/jmse12081411.
[15] X. Jiang *et al.*, "MFPA-Net: An efficient deep learning network for automatic ground fissures extraction in UAV images of the coal mining area", *International Journal of Applied Earth Observation and Geoinformation*, vol. 114, art. 103039, 2022. DOI: 10.1016/j.jag.2022.103039.
[16] W. Luo, M. Hao, S. Chen, Z. Zhang, P. Wang, and J. Li, "A positional knowledge-guided multiscale Gaussian detail enhancement deep learning network for ground fissure extraction", *IEEE Journal of Selected Topics in Applied Earth Observations and Remote Sensing*, vol. 17, pp. 13881–13892, 2024. DOI: 10.1109/JSTARS.2024.3417931.
[17] Y. Yuan, N. Zhang, C. Han, and D. Liang, "Automated identification of fissure trace in mining roadway via deep learning", *Journal of Rock Mechanics and* Geotechnical *Engineering*, vol. 15, no. 8, pp. 2039–2052, 2023. DOI: 10.1016/j.jrmge.2022.12.018.
[18] W. Pathonsuwan *et al.*, "RS-MSConvNet: A novel end-to-end pathological voice detection model", *IEEE Access*, vol. 10, pp. 120450–120461, 2022. DOI: 10.1109/ACCESS.2022.3219606.
[19] L. Liu, Y. Luo, X. Shen, M. Sun, and B. Li, "*β*-dropout: A unified dropout", *IEEE Access*, vol. 7, pp. 36140–36153, 2019. DOI: 10.1109/ACCESS.2019.2904881.
[20] J. Xie *et al.*, "Advanced dropout: A model-free methodology for Bayesian dropout optimization", *IEEE Transactions on Pattern Analysis and Machine Intelligence*, vol. 44, no. 9, pp. 4605–4625, 2022. DOI: 10.1109/TPAMI.2021.3083089.
[21] S. Sawaguchi and H. Nishi, "Slightly-slacked dropout for improving neural network learning on FPGA", *ICT Express*, vol. 4, no. 2, pp. 75–80, 2018. DOI: 10.1016/j.icte.2018.04.006.